Journal of *Marine Science and Engineering*

MDPI

Article

Spudcan Deep Penetration in Multi-Layered Soils Incorporating Sand Relative Density

Jun Zhao [1,2,*], Qingyun Zhu [1], Wenjing Huang [1], Yang Zhang [2,3] and Luyu Liu [4]

[1] Department of Offshore Oil and Gas Engineering, College of Petroleum Engineering, Xi'an Shiyou University, Xi'an 710065, China
[2] Shandong Marine Aerospace Equipment Technological Innovation Center, Ludong University, Yantai 264000, China
[3] Department of Naval Architecture and Ocean Engineering, Ulsan Ship and Ocean College, Ludong University, Yantai 264000, China
[4] Yantai CIMC Blue Ocean Technology Co., Ltd., Yantai 264000, China
* Correspondence: junzhao@xsyu.edu.cn

Abstract: Installing a spudcan jack-up rig in sediments with an interbedded sand-over-clay soil profile is still challenging in the offshore industry due to possible punch-through failure. The current methods for predicting the punch-through of spudcan usually ignore sand relative density, which is one of the most important parameters for sand soil. For multi-layered soils with interbedded sand commonly met in the field, this paper aims to determine the effects of sand relative density on predicting the punch-through failure of spudcan. Modified Mohr-Coulomb (MMC) and extended Tresca models characterized by incorporating a variation of mobilized strength parameters were used to describe the mechanical behaviors of sand and clay. Besides four groups of centrifuge tests, one field case in the South China Sea was also numerically simulated to validate the large deformation finite element (LDFE) analyses conducted in this paper. The results showed that neglect of sand relative density may lead to underestimation of the potential for punch-through failure of spudcan.

Keywords: jack-up rig; spudcan; bearing capacity; punch-through; relative density of sand

check for updates

Citation: Zhao, J.; Zhu, Q.; Huang, W.; Zhang, Y.; Liu, L. Spudcan Deep Penetration in Multi-Layered Soils Incorporating Sand Relative Density. *J. Mar. Sci. Eng.* **2023**, *11*, 33. https://doi.org/10.3390/jmse11010033

Academic Editor: Antoni Calafat

Received: 19 November 2022
Revised: 15 December 2022
Accepted: 22 December 2022
Published: 27 December 2022

Copyright: © 2022 by the authors. Licensee MDPI, Basel, Switzerland. This article is an open access article distributed under the terms and conditions of the Creative Commons Attribution (CC BY) license (https://creativecommons.org/licenses/by/4.0/).

1. Introduction

Self-elevating jack-up rigs have been widely used in shallow water to moderate water depths for offshore drilling and exploration, as well as wind turbine installation. In the stratified deposits with interbedded strong-over-soft soil, a punch-through failure of spudcan may occur, which is characterized by a sudden uncontrolled penetration into the underlying soft soils. Such a failure could lead to buckling of the leg, and even toppling of the whole unit, seriously threatening the safety of the jack-up rig. An average rate of one punch-through accident per year has been reported by Osborne and Paisley [1], which equates to an economic loss of between USD 1 million and USD 10 million (per accident) due to rig damage and loss of drilling time. The punch-through failure of spudcan continues to be prevalent in recent years [2], and the trend is rising due to the more complex soil conditions encountered in the field. For instance, the Sunda Shelf, Australia's Bass Strait and the North-West Shelf, the Gulf of Thailand, the South China Sea, offshore India, and the Arabian Gulf are particularly problematic in terms of stratigraphy and soil types [3].

In sediments with interbedded sand-over-clay, accurate prediction of the potential punch-through failure of spudcan is complicated by effects due to the nonlinear strength behavior and the phenomenon of progressive failure of the sand. The occurrence of a progressive failure in loading tests and centrifugal tests concerning footings on granular soils has been observed by Yamaguchi et al. [4], Aiban et al. [5], and Perkins et al. [6]. Based on empirical relationships by Bolton [7,8], in which the effects of sand relative density and confining stress on operative friction and dilation angles were taken into

account, Lee et al. [9,10] and Hu et al. [11] incorporated strength-dilatancy relationships in predicting the peak penetration resistance of spudcan on sand overlying clay through an iterative procedure. Besides, large deformation finite element (LDFE) methods, such as Remeshing and Interpolating Technique with Small Strain (RITSS), Arbitrary Lagrangian-Eulerian (ALE), and Coupled Eulerian-Lagrangian (CEL) have been used to calculate the penetration resistance profile of spudcan [12–21]. Although the density effect on the mechanical behavior of sand is well known, it is not considered in the punching shear and projected area method recommended by industry guidelines [22] for predicting the peak resistance of spudcan on sand overlying clay soils. It has not been clearly characterized whether the sand relative density has effects on the potential of punch-through failure of spudcan. By comparing it with centrifuge test results, it has been shown that the current two approaches consistently underestimate the penetration resistance of spudcan [10,23,24], especially for the size of modern-day spudcans (of the order of 10–20 m in diameter).

For the sand involved in a field case, there is usually no specific value for the relative density, only qualitative description, such as (medium) dense or loose sand. To ensure the safety of the jack-up rig in such a case, determining the effects of sand relative density on the potential of punch-through failure is required, not only the peak resistance of spudcan. This paper reports the results from an extended investigation carried out through large deformation finite element (LDFE) analyses. The likelihood of the punch-through failure of spudcan with and without considering the effects of sand relative density is compared, to determine the effect of sand relative density on the potential for the punch-through failure of spudcan on both double and multi-layered soils with interbedded sand overlying non-uniform clay.

2. Numerical Analysis

2.1. FE Modeling

LDFE calculations were carried out using the Coupled Eulerian-Lagrangian (CEL) approach in Abaqus/Explicit. The soil was modeled as an Eulerian domain of 4D in diameter and discretized using eight-node linear brick hexahedron elements with reduced integration, denoted as EC3D8R. The spudcan was taken as a rigid body and discretized with six-node linear brick wedge elements C3D6. The element size of 0.025D around the spudcan was used to achieve numerical accuracy and efficiency [18,20,25]. Considering the axial symmetry, only a quarter of the domain was modeled, as shown in Figure 1.

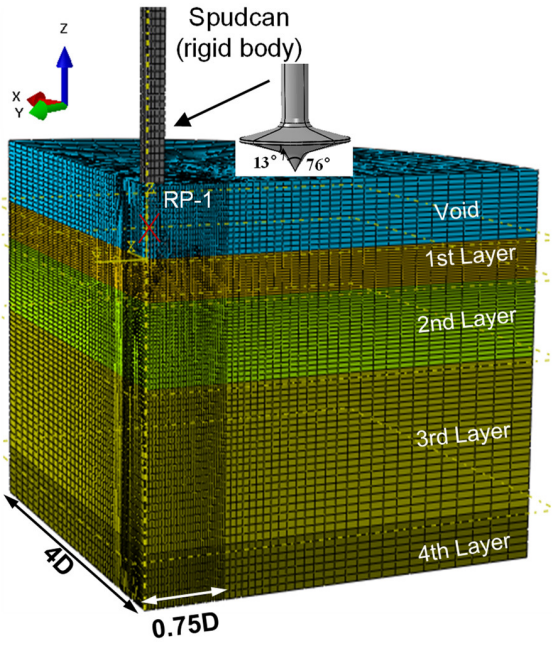


Figure 1. FE model of soil and spudcan.

The interaction between soil and spudcan was imposed using the 'general contact' algorithm, through a roughness factor of $\alpha = \frac{tan\delta}{tan\varphi'}$, where δ is the interface friction angle between the sand and spudcan, and φ' is the friction angle of the sand. A roughness factor of α = 0.5, within the range of 0.3–0.5 suggested by SNAME guidelines [22], was adopted in this study. The Poisson's ratio of v_{clay} = 0.49 was adopted for clay to simulate the undrained conditions, while v_{sand} = 0.3 for Poisson's ratio of the interbedded sand. For Young's modulus of sand and clay, values of E_{sand} = 50 MPa and E_{clay} = 350 × s_u were adopted. The bottom and lateral sides of the domain were constrained against flow in the normal direction, whereas the spudcan was constrained to move only in the vertical direction with a velocity of 0.2 m/s to simulate the penetration process.

2.2. Constitutive Models and Material Characteristics

2.2.1. Sand Layer

To simulate the progressive failure of the sand involved, the modified Mohr-Coulomb (MMC) model proposed by Zhao et al. [20] was adopted. Schematized in Figure 2 are the variations recommended to relate the shearing resistance angles, φ' and ψ', to the accumulated plastic shear strain of sand ξ_{sand}. A peak strength (P_p) was followed by a gradual reduction to the critical state (P_c). The two thresholds, ξ_p and ξ_c, corresponded to the peak and critical strength of sand, respectively. Similar sand models have been adopted by Potts et al. [26], Hu et al. [13], and Yapage et al. [27].

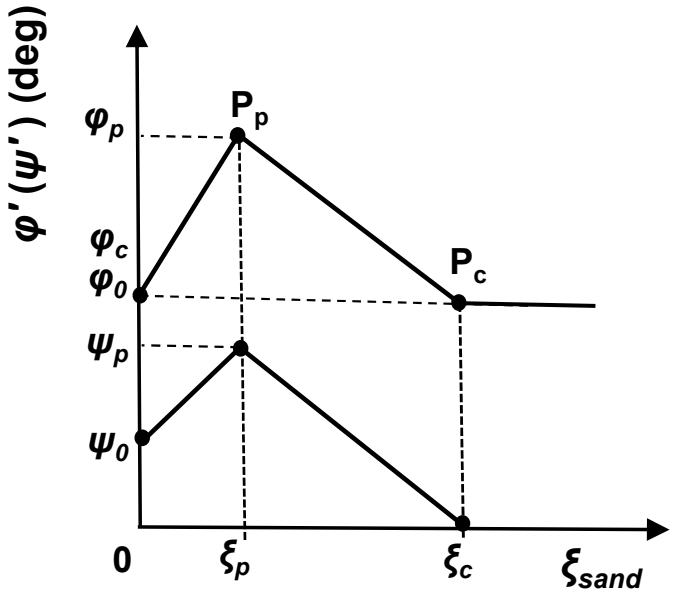


Figure 2. Variation of friction and dilation angles of modified Mohr-Coulomb model.

The peak friction angle φ_p and corresponding dilation angle ψ_p of sand can be determined by referencing the empirical strength-dilatancy correlations recommended by Bolton [7]:

$$\varphi_p - \varphi_c = mI_R \quad (1)$$

$$0.48\psi_p = \varphi_p - \varphi_c \quad (2)$$

$$I_R = I_D(10 - ln\ p') - 1 \quad (3)$$

where φ_c is the critical friction angle, m determines the enhancement of φ_p above φ_c due to dilatancy, with the suggested value of m = 3 for triaxial (and general) stress conditions, and I_R ($0 \leq I_R \leq 4$) is a relative dilatancy index. The mean stress in the sand layer during large-footings penetration is mostly lower than 150 kPa [13,28]. For p' in Equation (3), a

value of 150 kPa was suggested by Bolton [8] for any value less than 150 kPa, and the equation for I_R in Equation (3) was replaced with the following equation:

$$I_R = 5\ I_D - 1 \tag{4}$$

The accumulated plastic shear strain of sand ξ_{sand} (Figure 2) is defined as $\xi_{sand} = \sum \left| \frac{\sigma_1 \Delta\varepsilon_1^{pl} + \sigma_2 \Delta\varepsilon_2^{pl} + \sigma_3 \Delta\varepsilon_3^{pl}}{\overline{\sigma}} \right|$, where σ_i and $\Delta\varepsilon_i^{pl}$ (i = 1, 2, 3) are the stress components and incremental plastic strains measured from the start to the end of the current step, $\overline{\sigma}$ is the stress level index, and a value of 150 kPa [20] is adopted.

2.2.2. Clay Layer

For the underlying non-uniform clay involved, an extended Tresca model was adopted. The strain-softening effects were incorporated according to the accumulated shear strain ξ_{clay} as recommended by Einav and Randolph [29]. The current undrained shear strengths s_{uc} at the integration points were updated at the beginning of each time step as

$$s_{uc} = \left(\delta_{rem} + (1 - \delta_{rem}) e^{-3\xi_{clay}/\xi_{95}} \right) s_{u0} \tag{5}$$

where δ_{rem} is the ratio of fully remolded and intact strength (i.e., the inverse of the sensitivity, S_t), a value of S_t = 3 is adopted which falls within the typical range of S_t from 2 to 5 for marine clays [30–32]; ξ_{95} represents the value of ξ_{clay} required for soil to undergo 95% remolding, and a typical value of ξ_{95} = 12 within the range of 10 to 50 for marine clays is used [33]; $s_{u0} = s_{um} + kz$ is the intact undrained shear strength prior to any softening, s_{um} is the clay strength at the sand/clay interface, k is the strength gradient, and z represents the depth of clay. Considering the negligible elastic shear strain compared with the plastic shear strain in the LDFE analyses, the accumulated shear strain ξ_{clay} for the underlying clay were defined as

$$\xi_{clay} = \sum \left| \Delta\varepsilon_1^{pl} - \Delta\varepsilon_3^{pl} \right| \tag{6}$$

where $\Delta\varepsilon_1^{pl}$ and $\Delta\varepsilon_3^{pl}$ are the increments of maximum and minimum principal plastic strains, respectively.

2.3. Validation against Centrifuge Test Data

To validate the numerical model, four centrifuge tests named FS13, T1, H3C14, and FS9 were numerically recalculated, in which sands with different relative densities I_D were used. In tests T1 and H3C14, a dense sand layer (T1: silica sand with I_D = 85% and H3C14: silica sand with I_D = 74%) overlayed a non-uniform clay with different strength gradients of 1.2 kPa/m and 1.51 kPa/m. Test FS13 was carried out on a dense sand layer (silica sand with I_D = 89%) sandwiched by two non-uniform clay layers with a strength gradient of k = 0.75. In test FS9, a four-layer deposit of soft clay-sand-soft clay-stiff clay (silica sand with I_D = 44%) was used. The soil parameters used in the centrifuge tests are listed in Table 1.

For tests FS13, T1, H3C14, and FS9, corresponding LDFE analyses were conducted, namely FS13−FE−2nd−Id89, T1−FE−1st−Id85, H3C14−FE−1st−Id74, and FS9−FE −2nd−Id44, respectively (Table 2). The experimentally measured and numerically computed penetration resistance profiles are compared in Figure 3. For the key features of the full penetration resistance profile that position d_{peak} and magnitude q_{peak} of the peak resistance, the numerical predictions showed reasonable agreement with the corresponding centrifuge test results. For post-peak resistance, the computed profiles were lower than the measured profiles, especially for tests FS9 and T1. This may partly be due to the simplification in the sand model used. However, it is believed that the accuracy of the present numerical model was acceptable as this study is aimed to determine the effects of sand relative density on the potential for spudcan punch-through failure, which can be reflected by differences between the resistance profiles.

Table 1. Soil properties used in centrifuge tests.

Test	1st Layer				2nd Layer			Reference *
	$t1$(m)	I_D (%)	φ_c (°)	γ'(kN/m^3)	s_{um} (kPa)	γ' (kN/m^3)	k (kPa/m)	
T1 (D = 6 m)	3	85	34	10.8	6.0	6.5	1.2	Teh et al. [34]
H3C14 (D = 8 m)	3.03	74	31	10.6	11.31	6.5	1.51	Hu [14]
FS13 (D = 6 m)	1st layer				2nd layer			Hossain [3]
	$t1$(m)	s_{um} (kPa)	$\gamma\prime$ (kN/m^3)	$k1$ (kPa/m)	$t2$(m)	I_D (%)	φ (°)	$\gamma\prime$ (kN/m^3)
	3.7	0.5	6.5	0.75	2	89	34	10.0
	3rd layer				/			
	$t3$(m)	s_{um} (kPa)	$\gamma\prime$ (kN/m^3)	$k3$ (kPa/m)				
	20.8	4.775	6.5	0.75				
FS9 (D = 12 m)	1st layer				2nd layer			
	$t1$(m)	s_{um} (kPa)	$\gamma\prime$ (kN/m^3)	$k1$ (kPa/m)	$t2$(m)	I_D (%)	φ (°)	$\gamma\prime$ (kN/m^3)
	3	8	6.5	0	6	44	34	10.2
	3rd layer				4th layer			
	$t3$(m)	s_{um} (kPa)	$\gamma\prime$ (kN/m^3)	$k3$ (kPa/m)	$t4$(m)	s_{um} (kPa)	$\gamma\prime$ (kN/m^3)	$k4$ (kPa/m)
	11.52	8	6.5	0	3.96	37	6.5	0

* Reference, the literature from which the centrifuge tests were reported.

Table 2. Summary of LDFE analyses.

No.	Name	Sand							Clay *		Remarks
		t_s (m)	t_s/D	φ_p (Deg)	φ_c (Deg)	ψ_p (Deg)	ξ_p	ξ_c	s_{um} (kPa)	k (kPa/m)	
1	H3C14−FE−1st−Id74	3.03	0.38	39.1	31	16.8	0.01	0.4	11.31	1.51	
2	H3C14−FE−1st−L			/	31	/	/	0			
3	T1-FE−1st− Id85	3	0.5	43.8	34	20.3	0.01	0.4	6	1.2	
4	T1−FE −1st−L			/	34	/	/	/			
5	FS13−FE−2nd−Id89	2	0.33	44.4	34	21.6	0.01	0.23	4.775	0.75	
6	FS13−FE −2nd−L			/	34	/	/	/			
7	FS9−FE −2nd−Id44	6	0.5	/	34	/	/	0	8	0	
8	F−2nd&5th−Id−u	4.7	0.26	31.8	25	14.1	0.01	0.4	50	0	2nd sand
		7.4	0.41	39.8	30	20.3	0.01	0.4	55	0	5th sand
9	F−2nd&5th−Id−l	4.7	0.26	/	25	/	/	/	50	0	2nd sand
		7.4	0.41	36.8	30	14.1	0.01	0.4	55	0	5th sand

* The clay underneath the sand layer.

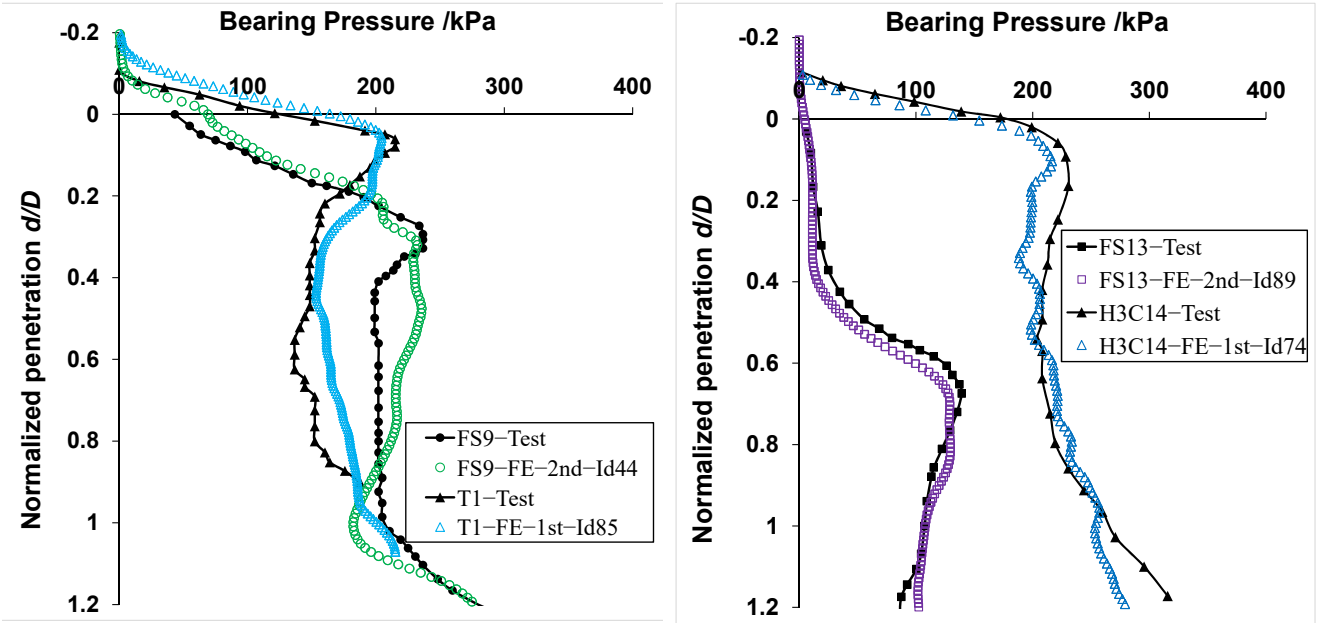


Figure 3. Comparison of resistance profiles of spudcan from centrifuge tests and numerical analyses: (**a**) test FS9 and T1; (**b**) test FS13 and H3C14.

3. Numerical Results

3.1. Interaction between Different Layers

The conventional punch-through of spudcan mainly focuses on double-layer strata. As stratified sediments with more than two layers commonly exists in the field, interactions between different layers during the spudcan deep penetrating process are inevitable. To visualize the soil movements involved, test FS9, previously conducted by Hossain [3] on four-layer soils of soft clay-sand-soft clay-stiff clay, was numerically simulated, as shown in Table 1.

In test FS9, underneath the 1st soft clay layer is a sand layer with a larger thickness (two times the 1st clay layer). For penetration through such a soft-overlying-strong soil profile, it is usually assumed that the overlaid soft layer will be completely squeezed out before achieving spudcan at the top of the underlying stronger layer. However, a different observation was clearly shown by the numerical simulations, which is in accordance with the corresponding centrifuge observation. As shown in Figure 4a, a soil plug consisting of soft clay from the 1st clay layer was trapped underneath the spudcan during penetration through the 1st soft clay layer, and moved forward with the spudcan into the underlying stronger sand layer. The shear band progressively transferred from the 1st clay layer to the underlying layers during the continuous penetration process. The direction of the trajectory of soil movement gradually changed from downward to horizontal, approaching the top of the underlying stronger layer, which is known as the squeezing phenomenon. The clay soil underneath the spudcan was gradually squeezed outside after a certain penetration.

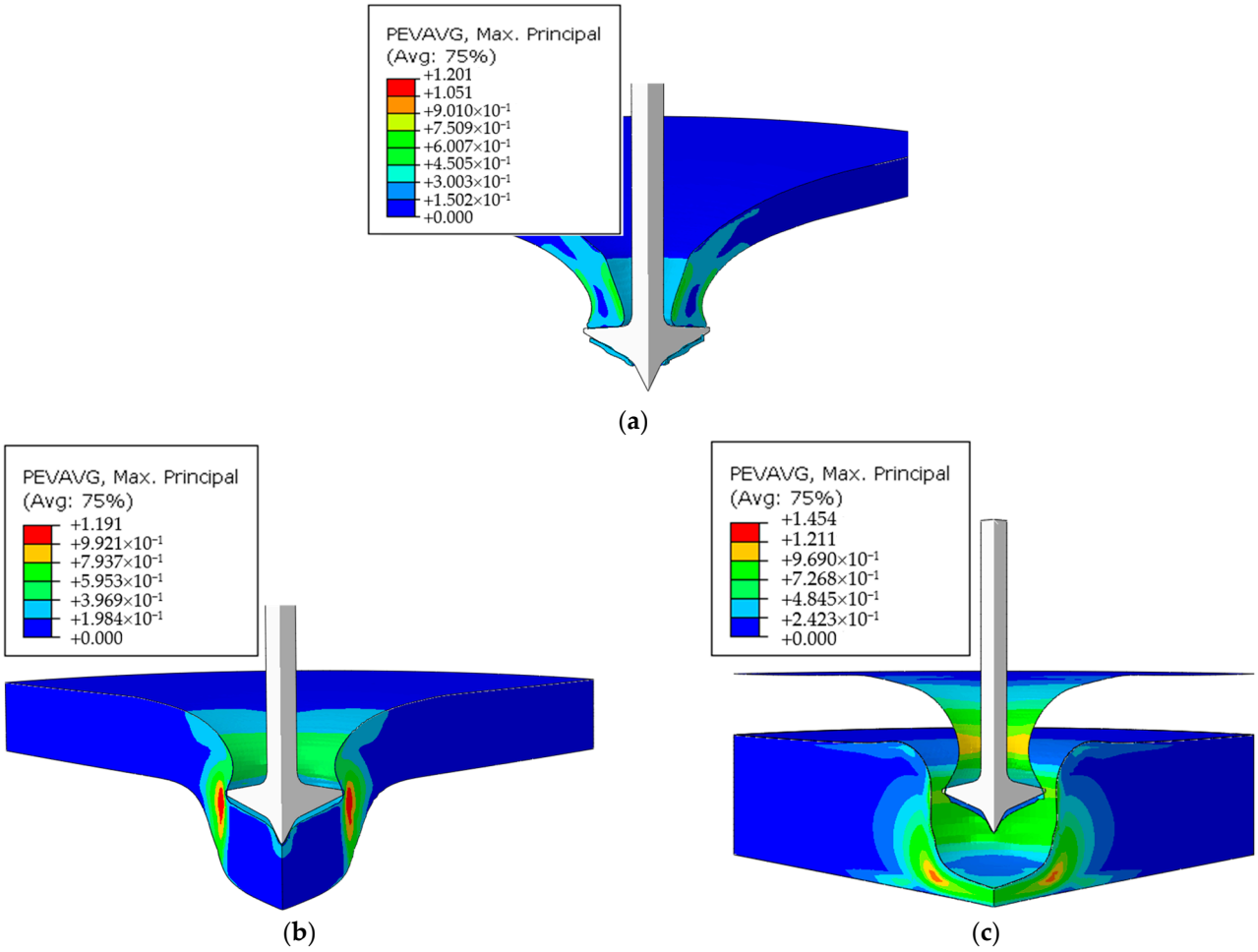


Figure 4. Plastic strain (PE) contours for simulation of centrifuge test FS9: (**a**) 1st clay layer; (**b**) 2nd sand layer; (**c**) 3rth clay layer.

The plastic failure emerged and gradually extended into the 2nd sand layer. The shear band initially extended outside and then transferred to incline inwards until it spread vertically along the periphery of the spudcan into the underlying 3rd soft clay layer. Underneath the clay plug, soil from the 2nd sand layer was trapped during penetrating, which is known as the sand plug (Figure 4b). The soil plugs trapped beneath the spudcan moved downwards together with the spudcan. As a result, the bottom of the 2nd sand layer was gradually pushed downwards into the 3rd soft clay layer below; the certain deformation of the 3rd layer can be seen in Figure 4c where the spudcan is still far from the interface between the 2nd sand and 3rd clay layers. Soil from the 3rd clay layer underneath the sand plug began to move outwards when the spudcan approached the interface between the 2nd sand and 3rd clay. The initial top of the 3rd clay layer had already been pushed downwards a certain distance by the sand plug underneath the spudcan. In the subsequent penetration, the 3rd clay layer was continuously squeezed, and the thickness of the 3rd clay layer underneath the sand plug became thinner until the center part was gradually squeezed out from the base of the sand plug.

3.2. Effects of Relative Density of Sand

In contrast to FS13–FE–2nd–Id89, T1–FE–1st–Id85 and H3C14–FE–1st–Id74 (Table 2), corresponding LDFE analyses with $\xi_c = 0$, namely no softening of sand, were conducted to investigate the effects of I_D on the potential for spudcan punch-through failure. The results of the penetration resistance profiles of spudcan were compared in Figure 5. The bearing pressure of spudcan, both q_{peak} and $q_{post\text{-}peak}$, given by LDFE analyses with $\xi_c = 0$ was lower

than that from the corresponding LDFE analyses, in which I_D was incorporated. It was shown that the penetration resistance of spudcan in sediments with interbedded sand, both q_{peak} and $q_{post\text{-}peak}$, would be underestimated without considering the influence of I_D.

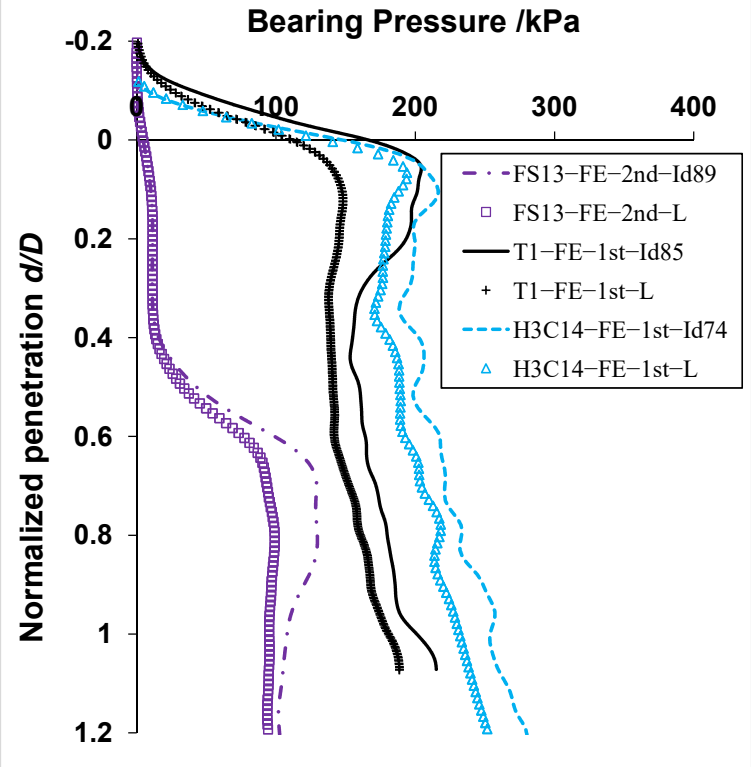


Figure 5. Comparison of penetration resistance profiles between cases using different sand relative density I_D.

Besides the centrifuge tests of FS13, T1, and H3C14, a field case in the South China Sea (named here as Location–1) was numerically analyzed to verify the influence of I_D of the interbedded sand layer on the prediction of spudcan penetration resistance, especially q_{peak} and $q_{post\text{-}peak}$. The soil stratigraphy was presented in Table 3. For the 2nd medium-dense sand, it was recommended that the value of I_D range from 35% to 65%, while a range of 65% to 85% was suggested for the 5th dense sand. In the LDFE analysis of F–2nd&5th–Id–u (Table 2), the upper limits of I_D of the 2nd and 5th sand layer were adopted, while the lower limits of I_D were used in F–2nd&5th–Id–L (Table 2). The numerical predictions of spudcan penetration resistances from F–2nd&5th–Id–u and F–2nd&5th–Id–L are compared in Figure 6, together with a diagrammatic sketch of the spudcan.

Table 3. Properties of seabed soils at the Location–1.

Stratum	Penetration (m)		γ' (kN/m^3)	s_u (kPa)	φ (Deg)	Soil Description
	From	To				
1	0.0	4.0	7.0	7.0	/	
2	4.0	8.7	8.7	/	25	medium dense fine sand
3	8.7	12.9	8.0	50.0	/	
4	12.9	14.0	8.0	75.0	/	
5	14.0	21.4	9.2	/	30	dense fine sand
6	21.4	40.3	8.8	55.0	/	

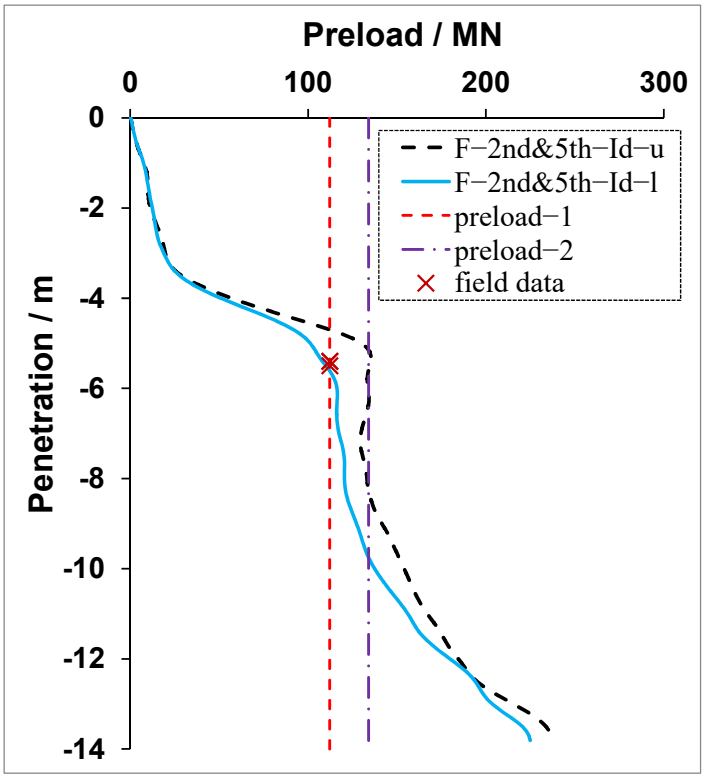


Figure 6. Comparison of penetration resistance profiles of spudcan at a field site.

Under the maximum preload of 112.2 MN, the ultimate penetration depth ranges between 4.7 m were given by F–2nd&5th–Id–u and 5.6 m by F–2nd&5th–Id–L. It was shown that the numerical predictions fit well with the field records of 5.4 m, 5.4 m, and 5.5 m for the three legs. The penetration resistance of the spudcan given by F–2nd&5th–Id–u is obviously larger than that from F–2nd&5th–Id–L, especially q_{peak}. Besides, there was no distinct $q_{post\text{-}peak}$ in the resistance profile from F–2nd&5th–Id–L, which was different from the upper limit resistance profile given by F–2nd&5th–Id–u. That is, a likely punch-through failure of the spudcan was shown by F–2nd&5th–Id–u (under a larger preload, e.g., preload-2 in Figure 6), while no clear potential for punch-through failure was indicated by F–2nd&5th–Id–L (without considering the influence of I_D).

To further verify the influence of I_D of the interbedded sand on the severity of the punch-through failure, the degree of post-peak reduction $\lambda = \frac{\Delta q}{\left(\frac{d}{D}\right)s_{u,avg}}$, as defined in Figure 7, was calculated based on the results of the LDFE analyses conducted in this study. Values of q_{peak} and λ were given by the LDFE analyses of FS13–FE–2nd–Id89, T1–FE–1st–Id85, and H3C14–FE–1st_Id74 (Table 2), denoted as q_peak_Id and λ_Id in Figure 8 incorporating real (or upper limit) values of I_D of interbedded sands. Instead, values of q_peak_L and λ_L were obtained from FS13–FE–2nd– L, T1–FE–1st–L, and H3C14–FE–1st–L, in which lower limit value of I_D (for the 5th sand in the field case) or $\xi_c = 0$ (without regard to I_D) was adopted. In Figure 8, comparisons of q_{peak} and λ between with and without incorporating I_D of interbedded sand were presented. It can be seen that the values of λ_Id were obviously larger than that for λ_L, especially for dense sand (Figure 8b), though a relatively small deviation existed between q_peak_L and q_peak_Id (Figure 8a). This indicated that the neglect of I_D of interbedded sand layers can lead to underestimation of the potential punch-through of the spudcan.

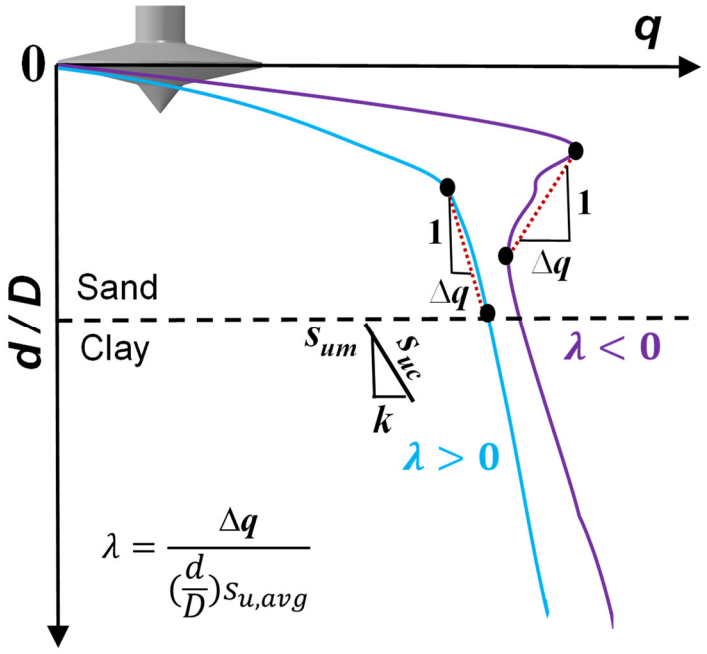
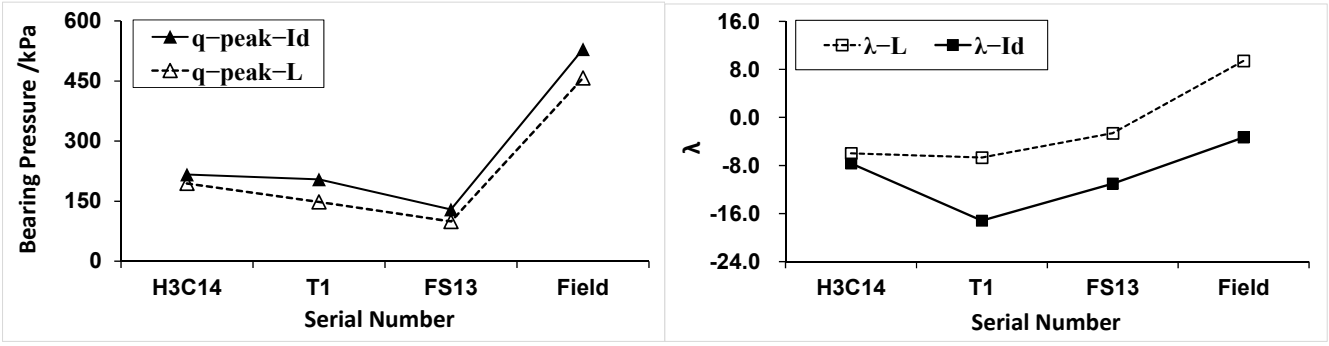


Figure 7. Definition of degree of post-peak reduction λ.



(**a**) (**b**)

Figure 8. Comparison of peak resistance q_{peak} and degree of post-peak reduction λ: (**a**) peak resistance q_{peak}; (**b**) degree of post-peak reduction λ.

4. Concluding Remarks

In sediments with an interbedded sand-over-clay soil profile, the punch-through failure of the spudcan can seriously affect the safety of jack-up rigs. Methods recommended in current guidelines for predicting the punch-through of the spudcan usually ignore sand relative density, which is one of the most important parameters for sand. By using a Coupled Eulerian-Lagrangian (CEL) approach in Abaqus/Explicit, a series of LDFE analyses, in which modified Mohr-Coulomb (MMC) and extended Tresca model were adopted, were conducted in this study to determine the effects of sand relative density on the potential for punch-through failure of the spudan. The following conclusions can be drawn from the results presented in this study.

(1) By incorporating the relative density of sand I_D, predictions of the penetration resistance profiles of the spudcan in sediments with interbedded sand-over-clay, especially peak resistance, fit well with measurements from centrifuge tests, as well as one field case conducted in the South China Sea.

(2) The numerical predictions of the penetration resistance of the spudcan, in which the sand relative density I_D was taken into account, are larger than those that did not consider I_D, especially peak resistance.

(3) A degree of post-peak reduction $\lambda = \frac{\Delta q}{\left(\frac{d}{D}\right)s_{u,avg}}$ was defined to further verify the influence of sand relative density I_D on the severity of the punch-through failure of the spudcan.

(4) The results of λ based on the LDFE analyses conducted in this study established that the relative density of sand I_D does indeed have effects on the punch-through failure of the spudcan, and ignoring I_D may underestimate the potential for punch-through.

Author Contributions: Conceptualization, J.Z.; methodology, J.Z.; software, J.Z., Q.Z. and L.L.; validation, J.Z., Q.Z. and W.H.; formal analysis, J.Z. and Q.Z.; investigation, J.Z., W.H., Y.Z. and L.L.; resources, J.Z., L.L. and Y.Z.; data curation, J.Z., W.H., Q.Z. and Y.Z.; writing—original draft preparation, J.Z.; writing—review and editing, J.Z., L.L. and Y.Z.; visualization, J.Z.; supervision, J.Z.; project administration, J.Z.; funding acquisition, J.Z. All authors have read and agreed to the published version of the manuscript.

Funding: This research was supported by the National Natural Science Foundation of China (Grant No. 51609201); the Natural Science Basic Research Program of Shaanxi Province (Grant No. 2020JQ-784) and the Open Project Program of Shandong Marine Aerospace Equipment Technological Innovation Center, Ludong University (Grant No. MAETIC2021-06).

Institutional Review Board Statement: Not applicable.

Informed Consent Statement: Not applicable.

Data Availability Statement: Not applicable.

Acknowledgments: The authors would like to thank the editors and reviewers for their many constructive suggestions and comments that helped improve the quality of the paper.

Conflicts of Interest: The authors declare no conflict of interest.

Abbreviations

d	penetration depth of spudcan base (lowest point at largest section)
D	diameter of generic spudcan at largest section
I_D	relative density of sand
k	strength gradient of clay (in kPa/m)
q_{peak}, $q_{post\text{-}peak}$	peak and post-peak penetration resistance of spudcan
s_{um}	intact undrained shear strength at top of clay
s_{u0}	intact undrained shear strength of soil
s_{uc}	current undrained shear strength of soil accounting for strain rate and softening
$s_{u,avg}$	undrained shear strength of clay averaged over $0.5D(L)$ below the sand-clay interface
t_s	thickness of sand layer
z	depth of the underlying clay
α	roughness factor of interaction between the spudcan and sand
γ'	effective unit weight of soil
φ_0, φ_p, φ_c	initial, peak, and critical friction angle of sand
ψ_0, ψ_p	initial and peak dilation angle of sand
ζ_{sand}, ζ_{clay}	accumulated plastic shear strain of sand and clay
ζ_p, ζ_c	thresholds corresponding to the peak and critical strength of sand
$\Delta\varepsilon_i^{pl}$ (i = 1, 3)	incremental plastic strains measured from start to end of current step
λ	degree of post-peak bearing reduction

References

1. Osborne, J.J.; Paisley, J.M. S E Asia jack-up punch-throughs: The way forward. In Proceedings of the International Conference on Offshore Site Investigation and Geotechnics Sustainability and Diversity, London, UK, 26–28 November 2002; pp. 301–306.
2. Hunt, R.J.; Marsh, P.D. Opportunities to Improve the Operational and Technical Management of Jack-up Deployments. *Mar. Struct.* **2004**, *17*, 261–273. [CrossRef]
3. Hossain, M.S. Experimental investigation of spudcan penetration in multi-layer clays with interbedded sand layers. *Geotechnique* **2014**, *64*, 258–277. [CrossRef]

4. Yamaguchi, H.; Kimura, T.; Fujii, N. On the influence of progressive failure on the bearing capacity of shallow foundation in dense sand. *Soils Found.* **1976**, *16*, 11–22. [CrossRef] [PubMed]
5. Aiban, S.A.; Znidarcic, D. Centrifugal modelling of bearing capacity of shallow foundations on sand. *J. Geotech. Eng.* **1995**, *121*, 704–712. [CrossRef]
6. Perkins, S.W.; Madson, C.R. Bearing capacity of shallow foundations on sand: A relative density approach. *J. Geotech. Geoenviron. Eng.* **2000**, *126*, 521–530. [CrossRef]
7. Bolton, M.D. The strength and dilatancy of sands. *Geotechnique* **1986**, *36*, 65–78. [CrossRef]
8. Bolton, M.D. Discussion: The strength and dilatancy of sands. *Geotechnique* **1987**, *37*, 219–226. [CrossRef]
9. Lee, K.K.; Cassidy, M.J.; Randolph, M.F. Bearing capacity on sand overlying clay soils: Experimental and finite element investigation of potential punch-through failure. *Geotechnique* **2013**, *63*, 1271–1284. [CrossRef]
10. Lee, K.K.; Randolph, M.F.; Cassidy, M.J. Bearing capacity on sand overlying clay soils: A simplified conceptual model. *Geotechnique* **2013**, *63*, 1285–1297. [CrossRef]
11. Hu, P.; Wang, D.; Cassidy, M.J.; Stanier, S.A. Predicting the resistance profile of a spudcan penetrating sand overlying clay. *Can. Geotech. J.* **2014**, *51*, 1151–1164. [CrossRef]
12. Qiu, G.; Grabe, J. Numerical investigation of bearing capacity due to spudcn penetration in sand overlying clay. *Can. Geotech. J.* **2012**, *49*, 1393–1407. [CrossRef]
13. Hu, P.; Wang, D.; Cassidy, M.J.; Stanier, S.A. Assessing the punch-through hazard of a spudcan on sand overlying clay. *Geotechnique* **2015**, *65*, 883–896. [CrossRef]
14. Hu, P. Predicting Punch-through Failure of a Spudcan on Sand Overlying Clay. Ph.D. Thesis, The University of Western Australia, Crawley, Australia, 2015.
15. Zhao, J.; Jang, B.S.; Duan, M.L. Investigation of spudcan continuous penetration in multi-layer sediments with interbedded sand-overlaid-clay soil profile. In Proceedings of the 25th International Offshore and Polar Engineering Conference, Kona, HI, USA, 21–26 June 2015.
16. Zhao, J.; Jang, B.S.; Duan, M.L.; Song, L.S. Simplified numerical prediction of the penetration resistance profile of spudcan foundation on sediments with interbedded medium-loose sand layer. *Appl. Ocean Res.* **2016**, *55*, 89–101. [CrossRef]
17. Zhao, J.; Jang, B.S.; Duan, M.L. On spudcan deep penetration using Eulerian finite element in multi-layer sediments: Soil plug mechanism. *Ships Offshore Struct.* **2017**, *12*, 715–721. [CrossRef]
18. Zheng, J.; Hossain, M.S.; Wang, D. Numerical investigation of spudcan penetration in multi-layer deposits with an interbedded sand layer. *Geotechnique* **2017**, *67*, 1050–1066. [CrossRef]
19. Ullah, S.N.; Hu, Y. Peak punch-through capacity of spudcan in sand with interbedded clay: Numerical and analytical modelling. *Can. Geotech. J.* **2017**, *54*, 1071–1088. [CrossRef]
20. Zhao, J.; Jang, B.-S.; Duan, M.L.; Liang, C. A finite element approach for predicting the full resistance profile of a spudcan deeply penetrating in dense sand overlying clay. *Appl. Ocean Res.* **2019**, *87*, 155–164. [CrossRef]
21. Zhao, J.; Zhang, Y.; Liu, L. On cubic spudcan deep penetration in dense sand overlying non-uniform. *Clay. J. Mar. Sci. Eng.* **2022**, *10*, 1607. [CrossRef]
22. SNAME. *Guidelines for Site Specific Assessment of Mobile Jack-Up Units*; T & R Bulletin 5-5 and 5-5A; SNAME: Houston, TX, USA, 2008.
23. Cassidy, M.J.; Li, J.H.; Hu, P.; Uzielli, M.; Lacasse, S. Deterministic and probabilistic advances in the analysis of spudcan behaviour. In Proceedings of the 3rd International Symposium on Frontiers in Offshore Geotechnics, Oslo, Norway, 10–12 June 2015; pp. 183–214.
24. Hu, P.; Stanier, S.A.; Wang, D.; Cassidy, M.J. A comparison of full profile prediction methods for a spudcan penetrating sand overlying clay. *Geotech. Lett.* **2015**, *5*, 131–139. [CrossRef]
25. Lee, J.M.; Kim, Y.H.; Hossain, M.S.; Cassidy, M.J.; Hu, Y.; Park, S.C. Mitigating punch-through on sand-over-clay using skirted foundations. *Ocean Eng.* **2020**, *201*, 107133. [CrossRef]
26. Potts, D.M.; Dounias, G.T.; Vaughan, P.R. Finite element analysis of progressive failure of carsington embankment. *Geotechnique* **1990**, *40*, 79–101. [CrossRef]
27. Yapage, N.; Liyanapathirana, D.; Poulos, H.; Kelly, R.; Leo, C. Numerical modeling of geotextile-reinforced embankments over deep cement mixed columns incorporating strain softening behavior of columns. *Int. J. Geomech.* **2015**, *15*, 04014047. [CrossRef]
28. White, D.J.; Teh, K.L.; Leung, C.F.; Chow, Y.K. A comparison of the bearing capacity of flat and conical circular foundations on sand. *Geotechnique* **2008**, *58*, 781–792. [CrossRef]
29. Einav, I.; Randolph, M.F. Combining upper bound and strain path methods for evaluating penetration resistance. *Int. J. Numer. Methods Eng.* **2005**, *63*, 1991–2016. [CrossRef]
30. Kvalstad, T.J.; Nadim, F.; Harbitz, C.B. Deepwater geohazards: Geotechnical concerns and solutions. In Proceedings of the Offshore Technology Conference, Houston, TX, USA, 30 April–3 May 2001.
31. Andersen, K.H.; Jostad, H.P. Shear strength along inside of suction anchor skirt wall in clay. In Proceedings of the Offshore Technology Conference, Houston, TX, USA, 3–6 May 2004.
32. Randolph, M.F. Characterization of soft sediments for offshore applications. Keynote Lecture. In Proceedings of the 2nd International Conference on Site Characterization, Porto, Portugal, 19–22 September 2004; pp. 209–232.

33. Zhou, H.; Randolph, M.F. Resistance of full-flow penetrometers in rate-dependent and strain-softening clay. *Geotechnique* **2009**, *59*, 79–86. [CrossRef]
34. Teh, K.L.; Cassidy, M.J.; Leung, C.F.; Chow, Y.K.; Randolph, M.F.; Quah, C. Revealing the bearing capacity mechanisms of a penetrating spudcan through sand overlying clay. *Geotechnique* **2008**, *58*, 793–804. [CrossRef]

Disclaimer/Publisher's Note: The statements, opinions and data contained in all publications are solely those of the individual author(s) and contributor(s) and not of MDPI and/or the editor(s). MDPI and/or the editor(s) disclaim responsibility for any injury to people or property resulting from any ideas, methods, instructions or products referred to in the content.